

# Two-Layer Model Predictive Battery Thermal and Energy Management Optimization for Connected and Automated Electric Vehicles\*

Mohammad Reza Amini<sup>1</sup>, Jing Sun<sup>1</sup>, and Ilya Kolmanovsky<sup>2</sup>

**Abstract**—Future vehicles are expected to be able to exploit increasingly the connected driving environment for efficient, comfortable, and safe driving. Given relatively slow dynamics associated with the state of charge and temperature response in electrified vehicles with large batteries, a long prediction/planning horizon is needed to achieve improved energy efficiency benefits. In this paper, we develop a two-layer Model Predictive Control (MPC) strategy for battery thermal and energy management of electric vehicle (EV), aiming at improving fuel economy through real-time prediction and optimization. In the first layer, the long-term traffic flow information and an approximate model reflective of the relatively slow battery temperature dynamics are leveraged to minimize energy consumption required for battery cooling while maintaining the battery temperature within the desired operating range. In the second layer, the scheduled battery thermal and state of charge (SOC) trajectories planned to achieve long-term battery energy-optimal thermal behavior are used as the reference over a short horizon to regulate the battery temperature. Additionally, an intelligent online constraint handling (IOCH) algorithm is developed to compensate for the mismatch between the actual and predicted driving conditions and reduce the chance for battery temperature constraint violation. The simulation results show that, depending on the driving cycle, the proposed two-layer MPC is able to save 2.8 – 7.9% of the battery energy compared to the traditional rule-based controller in connected and automated vehicle (CAV) operation scenario. Moreover, as compared to a single layer MPC with a long horizon, the two-layer structure of the proposed MPC solution reduces significantly the computing effort without compromising the performance.

## I. INTRODUCTION

Efficient thermal management in electrified vehicles, including pure electric vehicles (EVs), hybrid electric vehicles (HEVs), and plug-in HEVs (PHEVs) is a significant factor in the overall vehicle energy consumption optimization. For EVs, cooling the battery pack in hot summer days takes substantial amount of energy, which can significantly compromise energy efficiency and driving range of pure EVs [1]. Moreover, since the required power for cooling the battery pack is delivered by the battery itself, the operation of the battery thermal management (BTM) system directly interacts with other power loads, such as the traction power, forming intricate feedback loops. Therefore, optimizing the battery

pack operating temperature during hot weather is essential for improving the overall vehicle energy efficiency.

There are few works in the open literature dedicated to optimization of the EVs' BTM system, see [2] for an overview. The Pontryagin's maximum principle is used in [3] to optimize the battery thermal and energy management dynamics. In a similar study [4], the dynamic programming (DP) approach has been used to find the global optimal solution for the BTM optimization problem. Both [3] and [4] have shown the benefits of using optimization in minimizing the required cooling power to maintain the battery temperature within the optimal operating range. However, such an optimization is usually carried out offline under the assumption that the whole driving cycle is known a priori.

While emerging connectivity and autonomous driving technologies are expected to provide unprecedented opportunities to improve mobility and safety, they also open up new dimensions for vehicle and powertrain control and optimization. Extensive studies have been carried out on fuel economy optimization for electrified vehicles [5]. However, the implications of the connected and automated vehicles (CAVs) operation on power and thermal management have not been fully explored for electrified vehicles. The CAV technology will allow for the incorporation of a range of new high-value information into the optimization process when determining the optimal energy flow and power split strategies under real-world driving conditions, thereby realizing the full (and hitherto unfulfilled) energy saving potential of electrified vehicles [6].

The thermal subsystem of an EV has several special characteristics and requirements that are relevant to predictive control. In particular, due to slow thermal dynamics, the optimization has to consider a long time horizon. Inspired by the recent works in the literature on multi-layer optimization and prediction for systems with different time scales, including those for microgrids [7] and building energy management systems [8], we propose and develop an innovative two-layer MPC formulation for battery thermal and energy management optimization in this paper. The proposed two-layer MPC cools the battery pack by keeping its temperature within a certain interval based on traffic conditions and vehicle power demand. Responding to the predicted traffic conditions provided by the CAV (V2V/V2I) environment, the proposed two-layer MPC manages the power used for cooling so that the powertrain system and associated subsystems operate efficiently to achieve overall system efficiency optimization for different driving scenarios.

The contribution of this paper is threefold. First, the

\*This paper is based upon the work supported by the United States Department of Energy (DOE), ARPA-E NEXTCAR program under award No. de-ar0000797.

<sup>1</sup>Mohammad Reza Amini and Jing Sun are with the Department of Naval Architecture & Marine Engineering, University of Michigan, Ann Arbor, MI 48109 USA. Emails: {mamini, jingsun}@umich.edu

<sup>2</sup>Ilya Kolmanovsky is with the Department of Aerospace Engineering, University of Michigan, Ann Arbor, MI 48109 USA. Email: ilya@umich.edu

energy saving potential of predictive BTM system in EVs is exploited by utilizing the traffic flow information over a long prediction horizon to account for relatively slow thermal dynamics of the battery. Second, a two-layer MPC framework is developed to not only reduce the computation complexity versus a single-layer MPC with a long horizon, but also to integrate the optimization of battery thermal and energy management into a hierarchical control framework to account for different time-scales of prediction and control at each layer. Third, an intelligent online constraint handling algorithm is developed and incorporated into the two-layer MPC structure to reduce the chances of the battery temperature constraint violation in the presence of the mismatch between the actual and predicted speed profiles, specifically when long range prediction is used.

## II. BATTERY THERMAL AND ELECTRICAL MODELS

To formulate an MPC for BTM system, both the electrical and thermal characteristics of the battery have to be captured by the prediction model. The thermal sub-model approximates the battery pack as a lumped mass ( $m_{bat}$ ) with heat capacity  $C_{th,bat}$ , and can be described as follows [3]:

$$\dot{T}_{bat}(t) = \frac{1}{m_{bat}C_{th,bat}}(I_{bat}^2 R_{bat} + \dot{Q}), \quad (1)$$

where,  $T_{bat}$ ,  $I_{bat}$ , and  $R_{bat}$  are the battery temperature, current, and internal resistance, respectively.  $\dot{Q} < 0$  is the required heat flow rate for cooling the battery, and it is treated as the input to the battery thermal model in this paper.

The electric system sub-model of the battery includes the battery voltage ( $U_{bat}$ ), which can be expressed as a function of the open-circuit voltage ( $U_{oc}$ ),  $R_{bat}$ , and  $I_{bat}$  as follows:

$$U_{bat} = U_{oc} - I_{bat}R_{bat} \quad (2)$$

$U_{oc}$  and  $R_{bat}$  in (2) are functions of the battery state-of-charge ( $SOC$ ) and  $T_{bat}$ . The battery current can be written as a function of the total demanded power as follows:

$$I_{bat} = (P_{trac} + P_{temp})/U_{bat}, \quad (3)$$

where,  $P_{trac}$  is the demanded traction power, and  $P_{temp}$  is the required power to provide  $\dot{Q}$  for the BTM system. It is assumed in Eq. (3) that  $P_{trac}$  and  $P_{temp}$  are the main power loads on the battery, and other auxiliary loads on the battery are neglected. By substituting  $U_{bat}$  in (2) with  $(P_{trac} + P_{temp})/I_{bat}$  (Eq. (3)),  $I_{bat}$  can be re-written:

$$I_{bat}(t) = \frac{U_{oc} - \sqrt{U_{oc}^2 - 4R_{bat}(P_{trac} + P_{temp})}}{2R_{bat}} \quad (4)$$

Using (4), Eq. (1) becomes:

$$\dot{T}_{bat}(t) = \xi(T_{bat}(t)) = \frac{(U_{oc} - \sqrt{U_{oc}^2 - 4R_{bat}(P_{trac} + P_{temp})})^2}{4R_{bat}} + \dot{Q}}{m_{bat}C_{th,bat}}. \quad (5)$$

Moreover,  $SOC$  is governed by:

$$\dot{S}OC(t) = \zeta(SOC(t)) = -\frac{I_{bat}(t)}{C_{nom}} \quad (6)$$

where,  $C_{nom}$  is the nominal capacity of the battery.  $P_{temp}$  is modeled as a linear function of the heat flow rate  $\dot{Q}$  [3]:

$$P_{temp}(\dot{Q}) = a_c \dot{Q}, \quad \dot{Q} \leq 0, \quad a_c < 0 \quad (7)$$

where  $a_c$  is a constant. The parameters of the battery and vehicle dynamics are adopted from the Autonomie [9] software library for an electric vehicle.

## III. SINGLE-LAYER MPC FOR BATTERY THERMAL AND POWER MANAGEMENT

The traditional BTM system attempts to maintain the battery temperature at a specified level, without considering the traffic information. A setpoint within the optimal temperature range of the battery operation is selected and tracked. Since the battery temperature can increase rapidly due to aggressive vehicle acceleration and deceleration and BTM has limited bandwidth to respond, the desired battery temperature setpoint ( $T_{bat}^{s.p.}$ ) is usually selected well below the upper limit of the optimum operation range to assure that the temperature stays within the limit during transients. This conservative tracking approach designed for worst case scenarios without predictive traffic information, often leads to considerable extra energy consumed for battery cooling. To exploit the traffic information made available through CAVs, and to improve thermal efficiency, a model predictive controller is designed in this section to minimize the required battery cooling power, and maintain the battery temperature within the desired operation range.

1) **Problem Formulation:** In order to formulate the MPC, first the thermal ( $\xi$ ) and electric ( $\zeta$ ) models (Eqs. (6) and (5)) are discretized by applying the Euler forward method:

$$SOC(k+1) = f_{SOC}(k) = SOC(k) + T_s \zeta(SOC(k)), \quad (8)$$

$$T_{bat}(k+1) = f_{T_{bat}}(k) = T_{bat}(k) + T_s \xi(T_{bat}(k)), \quad (9)$$

where,  $T_s$  is the sampling time for control update (e.g.,  $T_s=1$  sec). We consider a single-layer MPC with an economic cost function formulated over a finite-time horizon ( $N$ ) with  $\dot{Q}$  being the optimization variable:

$$\begin{aligned} \min_{\dot{Q}(\cdot|k)} \quad & \sum_{i=0}^N P_{temp}(i|k), \\ \text{s.t.} \quad & T_{bat}(i+1|k) = f_{T_{bat}}(i|k), \quad i = 0, \dots, N, \\ & SOC(i+1|k) = f_{SOC}(i|k), \quad i = 0, \dots, N, \\ & T_{bat}^{LL} \leq T_{bat}(i|k) \leq T_{bat}^{UL}, \quad i = 0, \dots, N, \\ & 30\% \leq SOC(i|k) \leq 90\%, \quad i = 0, \dots, N, \\ & -3000 \text{ W} \leq \dot{Q}(i|k) \leq 0, \quad i = 0, \dots, N-1, \\ & T_{bat}(0|k) = T_{bat}(k), \quad SOC(0|k) = SOC(k), \end{aligned} \quad (10)$$

where,  $(i|k)$  designates the prediction for the time instant  $k + iT_s$  made at the time instant  $k$ . The nonlinear MPC optimization problem (10) attempts to minimize the power spent for battery thermal management  $P_{temp} = a_c \dot{Q}$  over the prediction horizon, while enforcing the state and input constraints.  $T_{bat}^{UL}$  and  $T_{bat}^{LL}$  are the upper and lower limits of the battery operating temperature, and they are set to  $40^\circ C$  and  $20^\circ C$ , respectively. Note that  $\dot{Q}$  is always negative for battery cooling scenario.  $f_{SOC}(k)$  and  $f_{T_{bat}}(k)$  are the discretized nonlinear dynamics of  $SOC$  and  $T_{bat}$  calculated according to (8) and (9). The optimization problem is solved at every time

step, then  $\dot{Q}(k)$  is commanded to the system and the horizon is shifted by one step ( $T_s$ ). The MPC simulation is carried out on a desktop computer, with an Intel® Core i7@2.60 GHz processor, in MATLAB®/SIMULINK® using YALMIP [10] for formulating the optimization problem, and IPOPT [11] for solving the optimization problem numerically.

2) **Performance Evaluation:** Intuitively, the solution of the optimization problem in (10) results in the battery temperature to be close to the upper limit  $T_{bat}^{UL}$  to minimize the cooling power consumption. However, since sudden changes in the  $P_{trac}$  could increase the battery temperature and cause  $T_{bat}$  to exceed the desired range, MPC with different prediction horizons will respond differently. Fig. 1 shows the results of applying the nonlinear MPC (10) with different prediction horizons ( $N$ ) on the EPA Urban Dynamometer Driving Schedule (UDDS), where it is assumed that the entire driving cycle is available, and the battery initial temperature ( $T_{bat,0}$ ) is the same in all the simulated runs. Additionally, the MPC simulation results are compared with simple rule-based (On/Off) controller which attempts to maintain  $T_{bat}$  at a constant level of  $T_{bat}^{s.p.}=35^\circ C$ .

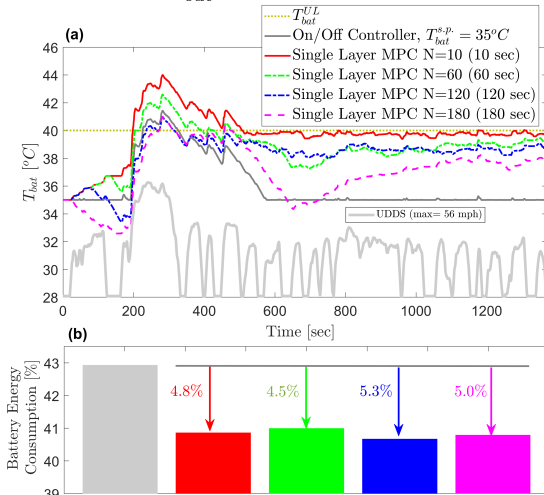


Fig. 1. The performance of the single layer MPC for battery thermal (a) and energy (b) management with different prediction horizons at  $T_{bat,0} = 35^\circ C$  for UDDS.

Fig. 1 shows that with a short prediction horizon ( $N=10$ ), the controller does not have enough lead time to take mitigating actions to prevent constraint violation caused by sudden increase in the traction power around  $t = 200$  sec. However, as the prediction horizon is being extended, the MPC takes proactive actions to reduce the temperature before the heating load increases around 200 sec, therefore significantly reducing the time for the battery to stay in over-temperature condition. As shown in Fig. 1-b, compared to the simple rule-based controller, 4.5 – 5.3% improvement in the energy consumption can be achieved by using the predictive controllers. The temperature upper limit violation, as expected, becomes less frequent as the prediction horizon being extended. When the horizon is longer than 120 sec, the MPC puts the efforts to decrease  $T_{bat}$  from the early seconds, which eventually results in both fuel saving ( $\geq 5\%$ ) and reduced constraint violation by up to 41% (compared to the rule-based controller).

3) **Robustness to Prediction Uncertainty:** This study confirms the advantages of incorporating the future traffic information for battery thermal and energy optimization via an MPC framework. Due to the large thermal inertia and therefore large time constant in the thermal response, however, BTM system requires much longer horizon information to capitalize on the benefits associated with the MPC approach.

On the other hand, the implementation of the MPC over a long horizon is not practical for two main reasons: (i) it is computationally demanding, and (ii) the accuracy in future traffic event prediction over a longer horizon cannot be guaranteed. The average computation time per iteration and execution for the single-layer MPC with  $N=10, 60, 120, 180$  sec was recorded as 0.75, 2.22, 6.24, 10.78 sec, respectively. It can be seen that the MPC with a long horizon is computationally expensive with average computation time exceeding the sampling time  $T_s=1$  sec. This clearly impedes the real-time implementation of the single-layer MPC. Moreover, vehicle speed profile can be accurately estimated using traffic and infrastructure information (V2I/V2X) only over a short horizon [12]. The prediction of the vehicle speed over an extended horizon is subject to uncertainties, which consequently affects the performance of the MPC for BTM over a long horizon.

While accurate long term vehicle speed prediction is difficult to obtain, it might not be necessary to claim most of the fuel saving benefits. We show in this paper that an approximate knowledge of future vehicle speed profile based on the average traffic flow velocity ( $V_{flow}$ ) estimation can be integrated into the single-layer MPC controller to reduce energy consumption.  $V_{flow}$  is estimated according to the approach proposed in [12], where the traffic flow data are extracted from a traffic monitoring system described in [13], exploiting the extensive coverage of the cellular network, GPS-based position and velocity measurements, and the communication infrastructure of cellphones. Fig. 2 illustrates the concept of the average traffic flow speed trajectory and compares it against the actual speed profile. It can be observed that the vehicle speed profile prediction is close to the actual speed for the first few cycles, before it merges into the average traffic flow speed (gray band) over the long horizon. For more details, see [12].

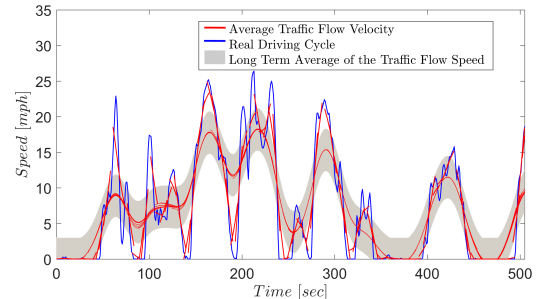


Fig. 2. The virtual traffic flow speed versus the actual driving cycle. In this paper, it is assumed that the traffic flow velocity information is repeatedly updated every cycle over a 250-sec window.

To understand the effects of uncertainties associated with the long prediction horizon, we consider the implementation

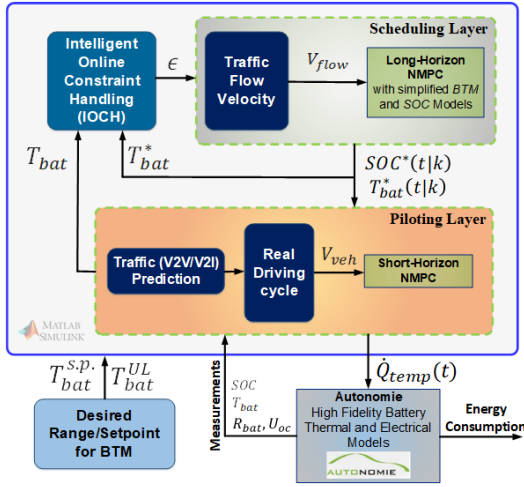


Fig. 3. Schematic of Two-Layer NMPC for battery thermal and energy management optimization.

of the single-layer MPC with both the actual speed profile, and with the one estimated from the traffic flow information. It was previously observed from Fig. 1 that the single-layer MPC with exact vehicle speed profile results in up to 5% saving in the battery energy compared to the rule-based controller. On the other hand, up to 3.9% energy saving is achieved when using traffic flow information, compared to 5% with the exact speed profile. Despite the mismatch between the real vehicle speed profile and long range prediction of the vehicle speed profile based on the traffic flow information, the energy saving is still substantial. Thus, the estimated long range vehicle speed profile via the traffic flow speed data can serve the purpose of the BTM system optimization.

#### IV. TWO-LAYER MPC FOR BATTERY THERMAL AND ENERGY OPTIMIZATION

It was observed that for the single-layer MPC, the maximum computation time per controller execution can reach as much as 20 *sec*, even on a powerful 2.60 GHz processor (note that  $T_s=1$  *sec*). In order to leverage the energy saving potentials of the long horizon traffic flow information and reduce the computation time of the MPC, we propose a two-layer MPC for battery thermal and energy optimization with a scheduling layer and a piloting layer as illustrated in Fig. 3. The scheduling layer has a relatively long horizon ( $H_l$ ), and the dynamic of the system is sampled at a slower rate ( $T_l > T_s$ ). The piloting layer has a short prediction horizon  $H_s$ , with a sampling time of  $T_s$ .

##### A. Scheduling Layer MPC with Long Horizon

In order to make the long-horizon MPC computationally efficient, the dynamic models for  $\dot{T}_{bat}$  and  $\dot{SOC}$  are simplified. To this end, first,  $I_{bat}$  equation from (4) is approximated by using the Taylor series expansion with different accuracies for  $SOC$  ( $I_{bat}^{SOC}$ ), and the current ( $I_{bat}^{T_{bat}}$ ) [3]:

$$I_{bat}^{SOC}(t) = \frac{a_c \dot{Q} + P_{trac}}{U_{oc}} + \frac{R_{bat}(a_c \dot{Q} + P_{trac})^2}{U_{oc}^3}, \quad (11)$$

$$I_{bat}^{T_{bat}}(t) = \frac{a_c \dot{Q} + P_{trac}}{U_{oc}}. \quad (12)$$

Next, Eqs. (11) and (12) are used to re-write the discretized battery state-of-charge ( $f_{SOC,l}$ ) and temperature ( $f_{T_{bat},l}$ )

dynamics over the long horizon  $H_l$  assuming the sampling time  $T_l$ , where  $SOC_l$  and  $T_{bat,l}$  designate the states of the simplified model used in the scheduling layer. The scheduling layer MPC is based on the following optimization problem formulation:

$$\begin{aligned} \min_{\dot{Q}(\cdot|k)} \quad & \sum_{i=0}^{H_l} P_{temp}(i|k), \\ \text{s.t.} \quad & \text{constraints listed in (10)}. \end{aligned} \quad (13)$$

The scheduling layer MPC optimizes  $\dot{Q}$  over the long horizon, and its solution is used to schedule the desired values of the battery temperature ( $T_{bat}^*$ ) and state-of-charge ( $SOC^*$ ) for the piloting layer. Note that the structure of the scheduling layer MPC is similar to the single-layer MPC in (10), but with a different sampling rate. This, as will be shown later, results in significantly reduced computational load.

##### B. Piloting Layer MPC with Short Horizon

$T_{bat}^*$  and  $SOC^*$  from the scheduling layer are passed on to the piloting layer, where these values are used by a short-horizon MPC for tracking. The output of the scheduling layer MPC is updated every  $T_l$ , during which the output of the short-horizon MPC is updated  $\tau = T_l/T_s$  times, where  $\tau \in \mathbb{Z}$  is the ratio between the long and short horizon length. The length of the scheduled values which need to be passed on to the piloting layer depends on the piloting layer prediction horizon ( $H_s$ ). Moreover, since  $T_l > T_s$ , the scheduled  $T_{bat}^*$  and  $SOC^*$  are passed on as piece-wise constant functions:  $T_{bat}^*(t|k)$  and  $SOC^*(t|k)$  [8].

The short-horizon MPC of the piloting layer is formulated as follows to track the scheduled  $T_{bat}^*$  and  $SOC^*$  references from the scheduling layer:

$$\begin{aligned} \min_{\dot{Q}(\cdot|k)} \quad & \sum_{j=0}^{H_s} \left\{ \begin{aligned} & (T_{bat}(j|k) - T_{bat}^*(j|k))^2 \\ & + w_1 (SOC(j|k) - SOC^*(j|k))^2 \end{aligned} \right\}, \\ \text{s.t.} \quad & T_{bat}(j+1|k) = f_{T_{bat}}(j|k), \quad j = 0, \dots, H_s, \\ & SOC(j+1|k) = f_{SOC}(j|k), \quad j = 0, \dots, H_s, \\ & -3000 \text{ W} \leq \dot{Q}(j|k) \leq 0, \quad j = 0, \dots, H_s - 1, \\ & T_{bat}(0|k) = T_{bat}(k), \quad SOC(0|k) = SOC(k). \end{aligned}$$

When performing optimization in the piloting layer, we assume that the vehicle speed and the demanded traction power can be estimated accurately over the short horizon. Moreover, the constraints on the battery temperature and  $SOC$  are not considered, as the long-horizon MPC has enforced these constraints in the scheduling layer. This will help to (i) reduce the computation time of the piloting layer optimization problem, (ii) avoid the infeasibility problem of the short-horizon MPC. Moreover, the computation times of the two-layer MPC at both layers are significantly lower than the single-layer MPC, because of:

- The larger sampling time used at the scheduling layer leading to substantially reduced optimization variables for the same prediction time window.
- Simplified dynamics of  $SOC_l$  and  $T_{bat,l}$ .
- Non-redundant constraint enforcement with the battery temperature constraint being enforced at the scheduling layer and removed from the piloting layer MPC.

### C. Intelligent Online Constraint Handling

Since the battery temperature constraint is removed from the short-horizon MPC, an intelligent online constraint handling (IOCH) algorithm is added to the structure of the two-layer MPC (shown in Fig. 3) to reduce the battery temperature limit violation that may be caused by the mismatch between the actual driving conditions and assumed driving conditions based on average traffic flow information. The IOCH block takes into account the violation of the battery temperature limits, and monitors the difference between  $T_{bat}$  and  $T_{bat}^*$ . The addition of the IOCH block introduces an extra optimization variable  $\epsilon$  which modifies the upper temperature bound at the scheduling layer to avoid temperature limit violations at the piloting layer, with consideration of the battery cooling power minimization. For this purpose, the cost function of the long-horizon MPC at the scheduling layer in Eq. (10) is modified as follows:

$$\min_{\hat{Q}(i|k), \epsilon(k)} \sum_{i=0}^{H_l} P_{temp}(i|k) + \gamma(\delta(T_{bat}, T_{bat}^{UL}) - \epsilon(i|k))^2, \quad (14)$$

where,  $\gamma$  is a weighting factor to adjust the controller effort for reducing the constraint violation. The long-horizon MPC is subject to the constraints listed in (13), except for  $T_{bat}(i|k)$ , which is now subject to:

$$\begin{aligned} T_{bat}^{UL}(i|k) &\leq T_{bat}^{UL} - \epsilon(i|k), \quad i = 0, \dots, H_l \\ \epsilon(i|k) &\geq 0, \quad i = 0, \dots, H_l - 1, \end{aligned} \quad (15)$$

where,  $T_{bat}^{UL}(i|k)$  denotes the variable upper limit of the battery temperature operation. The function  $\delta(T_{bat}, T_{bat}^*)$  in Eq. (14) is defined as follows:

$$\delta(T_{bat}, T_{bat}^{UL}) = \begin{cases} 0 & \text{if } T_{bat} \leq T_{bat}^{UL} \\ T_{bat} - T_{bat}^{UL} & \text{if } T_{bat} > T_{bat}^{UL} \end{cases} \quad (16)$$

Fig. 4 shows the performance of the two-layer MPC for UDDS at  $T_{bat,0} = 39^\circ\text{C}$ ,  $H_l = 180 \text{ sec}$ , and  $H_s = 15 \text{ sec}$ . It can be seen that when  $T_{bat}^{UL}$  is constant and set to be  $40^\circ\text{C}$ , the scheduled battery temperature trajectory ( $T_{bat}^*$ ) does not violate the upper limit constraint. But, the actual battery

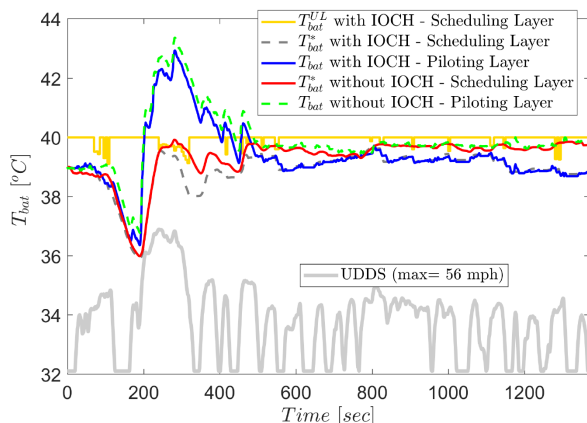


Fig. 4. The results of battery thermal management from Two-Layer MPC with and without IOCH for the UDDS ( $T_{bat}^{UL}=40^\circ\text{C}$ ,  $T_{bat,0}=39^\circ\text{C}$ ).

temperature does because of the mismatch between the real and predicted driving cycle. However, by using Eq. (14) as the cost function of the scheduling layer MPC, the added optimization variable  $\epsilon$  modifies the upper limit (Eq. (15)) with respect to the mismatches between  $V_{flow}$  and  $V_{veh}$ , and reduces the overall  $T_{bat}^{UL}$  violation by 13%. It should be noted from Fig. 4 that compared to the two-layer MPC without IOCH, the energy saving results (as determined by terminal battery SOC) of the two-layer MPC with IOCH is 1% lower, which is expected, as the overall battery temperature is lower and constraint violations are less frequent. This is the price paid for putting more effort to maintain  $T_{bat}$  within the desired range. While temporary violations of  $T_{bat}^{UL}$  are tolerated, it is required that  $T_{bat}$  to be maintained within the optimum operating range to improve the battery life and health in long term [14].

### V. TWO-LAYER MPC SIMULATION RESULTS

In order to demonstrate the energy saving potentials of the proposed two-layer MPC for battery thermal management of electric vehicles, the predictive controller with IOCH is simulated for UDDS and the New York City Cycle (NYCC) at different initial battery temperature conditions. The NYCC features low speed stop-and-go traffic conditions. These results are compared with the traditional rule-based controller, and presented in Figs. 5-7. For UDDS, it can be seen from Fig. 5 that by the end of the driving cycle, the two-layer MPC reduces the drop in the battery SOC by 2.9% and 2.8% for  $T_{bat,0} = 35^\circ\text{C}$  and for  $T_{bat,0} = 39^\circ\text{C}$ , respectively, compared to the rule-based controller.

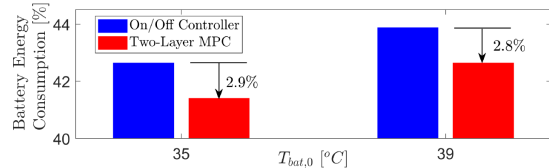


Fig. 5. The results of battery energy management by using Two-Layer MPC with IOCH and On/Off controller ( $T_{bat}^{s.p.}=35^\circ\text{C}$ ) for UDDS at  $T_{bat,0}=35^\circ\text{C}$  and  $39^\circ\text{C}$ .

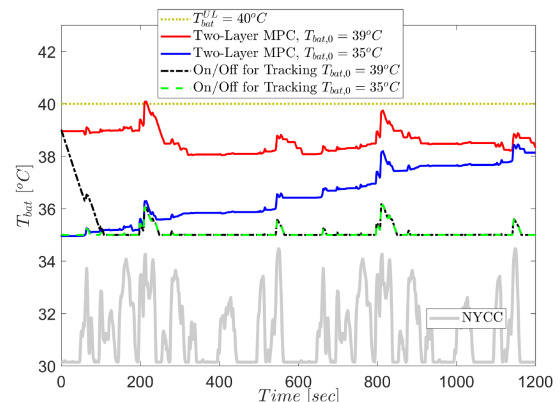


Fig. 6. The results of BTM by using Two-Layer MPC with IOCH and On/Off controller ( $T_{bat}^{s.p.}=35^\circ\text{C}$ ) for NYCC at  $T_{bat,0}=35^\circ\text{C}$  and  $39^\circ\text{C}$ .

For the NYCC, since the vehicle speed is low on average, aggressive rises in the demanded traction power and battery temperature are not observed. Thus, the two-layer MPC is able to maintain the battery temperature well below the upper limit, even with  $T_{bat,0} = 39^\circ\text{C}$ . By looking into

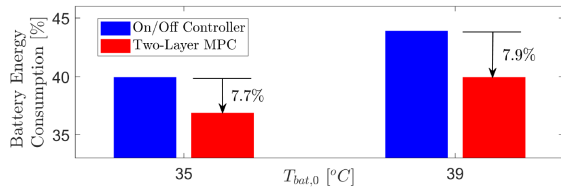


Fig. 7. The results of battery energy management by using Two-Layer MPC with IOCH and On/Off controller ( $T_{bat}^{s.p.}=35^{\circ}C$ ) for NYCC at  $T_{bat,0}=35^{\circ}C$  and  $39^{\circ}C$ .

the battery energy management results for the NYCC in Fig. 7, it can be seen that the conservative design of the rule-based controller results in a significant drop in the battery *SOC* by the end of the driving cycle. Compared to the rule-based controller, the two-layer MPC reduces battery energy consumption (as determined by terminal *SOC*) by 7.9% and 7.7% for  $T_{bat,0} = 39^{\circ}C$  and  $T_{bat,0} = 35^{\circ}C$ , respectively. This is because the rule-based controller tries to maintain the temperature at  $T_{bat}^{s.p.} = 35^{\circ}C$ , regardless of the traffic and driving conditions.

Finally, Table I summarizes the average and maximum required computation times for each layer of the two-layer MPC with and without IOCH. Also the average computation time of the single-layer MPC from Sec. III with a similar prediction horizon as of the scheduling layer MPC ( $N = H_l$ ), and  $T_s=1$  sec is listed in Table I. The average and maximum computation times of the scheduling layer MPC with and without IOCH are less than the sampling time ( $T_l=5$  sec). Moreover, it can be seen that in all cases, the average and maximum computation times of the piloting layer MPC is less than the sampling time  $T_s=1$  sec. Overall, it can be concluded that unlike the single-layer MPC, the two-layer MPC provides a computationally efficient framework.

TABLE I  
COMPUTATION TIME COMPARISON OF THE SINGLE-LAYER AND TWO-LAYER MPCs.

Controller	$T_{bat}^{UL} = 40^{\circ}C$	$T_{bat}^{UL} = variable$
<b>Single Layer MPC</b>	$N = 180$ sec	$T_s = 1$ sec
Average CPU Time	10.78 (sec)	N/A
<b>Scheduling Layer MPC</b>	$H_l = 180$ sec	$T_l = 5$ sec
Average CPU Time	0.855 (sec)	2.071 (sec)
Max CPU Time	1.396 (sec)	4.265 (sec)
<b>Piloting Layer MPC</b>	$H_s = 15$ sec	$T_s = 1$ sec
Average CPU Time	0.206 (sec)	0.197 (sec)
Max CPU Time	0.563 (sec)	0.780 (sec)

## VI. SUMMARY AND CONCLUSIONS

This paper investigates the design of a predictive and integrated battery thermal management (BMT) system in a connected and automated vehicles environment to improve energy efficiency and extend range of battery electric vehicles. To this end, first a single-layer MPC formulation was proposed to minimize the battery cooling power, while enforcing the battery temperature to be within the desired range. The simulation results showed that due to the relatively slow thermal dynamics of the battery, the MPC for BTM system requires information over a long horizon to achieve the design objectives. The simulation

results confirmed that inclusion of the long horizon vehicle speed profile leads to 3 – 8% saving in the total battery energy consumption, specifically for congested city driving cycles, e.g., NYCC. However, the single-layer MPC with a long horizon is computationally demanding. A two-layer MPC with an intelligent online constraint handling (IOCH) was then developed to (i) reduce the computation time as compared to the single-layer MPC, (ii) utilize the long-term traffic flow information along with the short-term vehicle speed predictions, and (iii) account for the mismatch between the actual vehicle speed profile and the predicted traffic flow speed used over the long horizon to reduce the overall battery temperature limit violation. The simulation results showed that the proposed two-layer MPC is able to achieve energy consumption reduction at a lower computational cost and without relying on the precise knowledge of the future vehicle speed profile. Moreover, while up to 2.9% energy saving was achieved for the UDDS, it was shown that for low-speed congested driving cycles, e.g., NYCC, higher energy saving can be achieved, and the two-layer MPC can save up to 7.9% of the battery energy.

## REFERENCES

- [1] M. Zolot, A. Pesaran, and M. Mihalic. Thermal Evaluation of Toyota Prius Battery Pack. 2002. SAE Technical Paper 2002-01-1962.
- [2] E. Kim, K. Shin, and J. Lee. Real-Time Battery Thermal Management for Electric Vehicles. In *ACM/IEEE 5th Int. Conference on Cyber-Physical Systems*, 2014. Berlin, Germany.
- [3] S. Bauer, A. Suchanek, and F. León. Thermal and Energy Battery Management Optimization in Electric Vehicles Using Pontryagin’s Maximum Principle. *Journal of Power Sources*, 246:808–818, 2014.
- [4] Y. Masoudi, A. Mozaffari, and N. Azad. Battery Thermal Management of Electric Vehicles: An Optimal Control Approach. In *ASME Dynamic Systems and Control Conf.*, 2015. Columbus, OH, USA.
- [5] J. Guanetti, Y. Kim, and F. Borrelli. Control of Connected and Automated Vehicles: State of the Art and Future Challenges. *Annual Reviews in Control*, 45:18–40.
- [6] H. Lim, W. Su, and C. Mi. Distance-Based Ecological Driving Scheme Using a Two-Stage Hierarchy for Long-Term Optimization and Short-Term Adaptation. *IEEE Trans. on Vehicular Technology*, 66(3):1940–1949, 2017.
- [7] S. Cominesi, M. Farina, L. Giulioni, B. Picasso, and R. Scattolini. A Two-Layer Stochastic Model Predictive Control Scheme for Microgrids. *IEEE Trans. on Control systems Technology*, 26(1):1–13, 2018.
- [8] A. Lefort, R. Bourdais, G. Ansanay-Alex, and H. Guéguen. Hierarchical Control Method Applied to Energy Management of a Residential House. *Energy and Buildings*, 64:53–61, 2013.
- [9] S. Halbach, P. Sharer, S. Pagerit, A. Rousseau, and C. Folkerts. Model Architecture, Methods, and Interfaces for Efficient Math-Based Design and Simulation of Automotive Control Systems. 2010. SAE Technical Paper 2010-01-0241.
- [10] J. Lofberg. YALMIP: A Toolbox for Modeling and Optimization in MATLAB. In *2004 IEEE Int. Symp. on Computer Aided Control Sys. Design*, 2004. New Orleans, LA, USA.
- [11] A. Wächter and L. Biegler. On the Implementation of an Interior-Point Filter Line-Search Algorithm for Large-Scale Nonlinear Programming. *Mathematical Programming*, 106(1):25–57, 2006.
- [12] C. Sun, F. Sun, X. Hu, J. Hedrick, and S. Moura. Integrating traffic velocity data into predictive energy management of plug-in hybrid electric vehicles. In *ACC*, 2015. Chicago, IL, USA.
- [13] J. Herrera, D. Work, R. Herring, X. Ban, Q. Jacobson, and A. Bayen. Evaluation of Traffic Data Obtained via GPS-Enabled Mobile Phones: The Mobile Century field experiment. *Transportation Research Part C: Emerging Technologies*, 18(4):568–583, 2010.
- [14] J. Neubauer and E. Wood. Thru-life Impacts of Driver Aggression, Climate, Cabin Thermal Management, and Battery Thermal Management on Battery Electric Vehicle Utility. *Journal of Power Sources*, 259:262–275, 2014.